INT. J. NUM. METH. HEAT FLUID FLOW, VOL. 5, 225–237 (1995)

INTEGRAL TRANSFORM METHOD FOR BOUNDARY LAYER EQUATIONS IN SIMULTANEOUS HEAT AND FLUID FLOW PROBLEMS

H. A. MACHADO AND R. M. COTTA

Mechanical Engineering Department, EE/COPPE/UFRJ, Universidade Federal do Rio de Janeiro, Cx. Postal 68.503, Rio de Janeiro, RJ-21945-970, Brasil

ABSTRACT

The two-dimensional steady boundary layer equations, for simultaneous heat and fluid flow within ducts, are handled through the generalized integral transform technique. The momentum and energy equations are integral transformed by eliminating the transversal coordinate and reducing the PDE's into an infinite system of coupled non-linear ordinary differential equations for the transformed potentials. An adaptively truncated version of this ODE system is numerically handled through well known initial value problem solvers, with automatic precision control procedures. The explicit inversion formulae are then recalled to provide analytic expressions for velocity and temperature fields and related quantities of practical interest. Typical examples are presented in order to illustrate the hybrid numerical analytical approach and its convergence behaviour.

KEY WORDS Integral transform technique Boundary layer equations

NOMENCLATURE

N, M	truncation orders of systems (12a,b), respectively,
N_i, M_i	normalization integrals, (8c,d),
$Nu(Z)$	local Nusselt number ($= h4r_w/k$),
$Nu_{av}(Z)$	average Nusselt number ($= h4r_w/k$),
p, p^*	pressure field, dimensional and dimensionless
Pe	Peclet number ($= Re \cdot Pr$),
Pr	Prandtl number,
r, R	transversal coordinate, dimensional and dimensionless,
r_w	half-distance between parallel-plates,
Re	Reynolds number,
$T(r, z)$	temperature distribution,
T_0	inlet temperature,
T_w	wall temperature,
u, U	longitudinal velocity component, dimensional and dimensionless,
u_0	inlet velocity,
$U_\infty(R)$	separated velocity distribution (3a)
U_m	average fluid velocity,
v, V	transversal velocity component, dimensional and dimensionless,
X^+	dimensionless axial coordinate, as defined in (19),
z, Z	axial coordinate, dimensional and dimensionless,

Greek

α	thermal diffusivity,
ε	relative errors in adaptive procedure, (18),
$\Theta(R, Z)$	dimensionless temperature distribution,
$\Theta_{av}(Z)$	fluid bulk temperature,
λ_i, μ_i	eigenvalues of problems (7) and (6), respectively,
$\Gamma_i(R), \psi_i(R)$	eigenfunctions of problems (7) and (6), respectively,
ν	kinematic viscosity,

Subscripts and superscripts

$-$	integral transformed quantities,
i, j, k	order from eigenvalues or eigenfunctions.

0961–5539/95/030225–13$2.00

Received December 1993
Revised February 1994

INTRODUCTION

The thermohydraulic design of heat exchange equipment, in various industrial applications, has taken advantage of the progress on the computational and mathematical capabilities for simulations of non-isothermal internal flows[1]. Forced convection problems of incompressible single phase flows are frequently encountered within this context, which are commonly modelled through the boundary layer equations in two or three dimensions, either in a laminar or turbulent regimen, depending on the specific situation. Different numerical approaches are available for the approximate solution of the boundary layer equations in simultaneous heat and fluid flow problems[2], based on variations of the well known finite difference and finite element methods. A number of previous contributions utilized such approaches in the numerical treatment of the classical simultaneously developing flow problem, inside regularly shaped channels like circular tubes and parallel plates[1,3]. None of these schemes provide an automatic global error control to within user prescribed accuracy, and can become prohibitively computer intensive for increasing precision requirements. Also, a true benchmark solution for this class of problem is not readily available, and numerical codes are generally validated through analytic fully developed region solutions or rough comparisons with previously reported numerical results for alternative discrete approaches.

Within the last few years, a hybrid numerical–analytical approach has been advanced for the solution of different classes of linear and non-linear diffusion and convection–diffusion problems, as compiled in Reference 4, denoted the generalized integral transform technique. Most recent contributions are aimed at the accurate solution of non-linear heat and fluid flow problems[5–15], which include problems with variable properties, moving boundaries, irregular geometries, non-linear source terms, non-linear boundary conditions, Navier–Stokes equations, and boundary layer equations as well.

Due to its hybrid nature, this approach offers global error control to within user prescribed accuracy and quite efficient computational performance for a wide variety of problems.

In a previous contribution[16], the problem of simultaneous heat and fluid flow inside channels was analytically handled through the integral transform approach, by applying a linearization procedure to the velocity problem and yielding a linear non-separable energy equation. The approximate analytic expressions were then compared against finite difference results for the complete non-linear problem, offering a validation of this extended Graetz-type solution. The problem of hydrodynamic development inside channels, governed by the full non-linear momentum equation in boundary layer formulation, was again treated[15] by the generalized integral transform technique, providing a hybrid numerical–analytical solution to this classical problem, including wall injection or suction. The convergence behaviour of the eigenfunction expansions was illustrated and previously reported numerical solutions were validated. The present work progresses further into the analysis of the boundary layer equations for simultaneous heat and fluid flow, through the integral transform method. The momentum and energy equations are integral transformed concurrently, based on specific auxiliary eigenvalue problems. Also, the approach in Reference 15 is refined in terms of computational performance, through explicit separation of fully developed solutions, and improved implementation of the adaptive procedure[4,8] for automatic reduction of the truncated ODE system order and control of the global relative error. Sets of benchmark results for this classical test problem, under prescribed uniform wall temperature condition, are then provided in both graphical and tabular form.

ANALYSIS

Hydrodynamically and thermally developing incompressible laminar flow of a Newtonian fluid between parallel-plates is considered, subjected to an uniform wall temperature and uniform inlet conditions, for both velocity and temperature fields. Physical properties are assumed

constant and viscous dissipation and free convection effects are considered negligible, although not a limitation for application of the present approach. Within the range of validity for the boundary layer hypothesis, the problem formulation in dimensionless form is written as:

Continuity:

$$\frac{\partial U(R,Z)}{\partial Z}+\frac{\partial V(R,Z)}{\partial R}=0 \qquad 0<R<1,\ Z>0 \tag{1a}$$

Z-momentum equation:

$$U\cdot\frac{\partial U}{\partial Z}+V\frac{\partial U}{\partial R}=-\frac{\mathrm{d}p^*}{\mathrm{d}Z}+\frac{1}{Re}\cdot\frac{\partial^2 U}{\partial R^2} \qquad 0<R<1,\ Z>0 \tag{1b}$$

Energy equation:

$$U\cdot\frac{\partial\theta}{\partial Z}+V\frac{\partial\theta}{\partial R}=\frac{1}{Pe}\cdot\frac{\partial^2\theta}{\partial R^2} \qquad 0<R<1,\ Z>0 \tag{1c}$$

with inlet and boundary conditions given, respectively, by:

$$U(R,0)=1 \tag{1d}$$

$$V(R,0)=0 \tag{1e}$$

$$\theta(R,0)=1 \tag{1f}$$

$$\left.\frac{\partial U}{\partial R}\right|_{R=0}=0 \tag{1g}$$

$$V(0,Z)=0 \tag{1h}$$

$$\left.\frac{\partial\theta}{\partial R}\right|_{R=0}=0 \tag{1i}$$

$$U(1,Z)=0 \tag{1j}$$

$$V(1,Z)=0 \tag{1k}$$

$$\theta(1,Z)=0 \tag{1l}$$

where various dimensionless groups are defined as:

$$R=\frac{r}{r_w} \tag{2a}$$

$$Z=\frac{z}{r_w} \tag{2b}$$

$$U=\frac{u}{u_0} \tag{2c}$$

$$V=\frac{v}{u_0} \tag{2d}$$

$$p^*=\frac{p}{\rho\cdot u_0^2} \tag{2e}$$

$$\theta=\frac{T-T_w}{T_0-T_w} \tag{2f}$$

$$Re = \frac{u_0 \cdot r_w}{\nu} \tag{2g}$$

$$Pr = \frac{\nu}{\alpha} \tag{2h}$$

$$Pe = Re \cdot Pr \tag{2i}$$

For improved computational performance in the solution of the velocity field, with respect to the direct procedure[15], the fully developed flow situation is separated from the complete potential, in the form:

$$U(R, Z) = U^*(R, Z) + U_\infty(R) \tag{3a}$$

where

$$U_\infty(R) = \tfrac{3}{2} \cdot (1 - R^2) \tag{3b}$$

This is a commonly used device in the integral transform approach[4,8], equivalent to the separation of the steady-state solution in a transient problem, which acts by filtering the equation source terms responsible for the slower convergence rates in non-homogeneous problems. For the temperature problem, in the present situation, fully developed conditions result in trivial solution. After substitution of the splitting-up scheme, (3a), the problem formulation is rewritten as:

$$\frac{\partial U^*(R, Z)}{\partial Z} + \frac{\partial V(R, Z)}{\partial R} = 0 \tag{4a}$$

$$(U^* + U_\infty) \cdot \frac{\partial U^*}{\partial Z} + V\left(\frac{\partial U^*}{\partial R} - 3R\right) = -\left(\frac{dp^*}{dz} + \frac{3}{Re}\right) + \frac{1}{Re}\frac{\partial^2 U^*}{\partial R^2} \tag{4b}$$

$$(U^* + U_\infty)\frac{\partial \theta}{\partial Z} + V\frac{\partial \theta}{\partial R} = \frac{1}{Pe}\frac{\partial^2 \theta}{\partial R^2} \tag{4c}$$

and the inlet and boundary conditions for the longitudinal velocity component become:

$$U^*(R, 0) = 1 - U_\infty(R) \tag{4d}$$

$$\left.\frac{\partial U^*}{\partial R}\right|_{R=0} = 0 \tag{4e}$$

$$U^*(1, Z) = 0 \tag{4f}$$

while the other conditions remain unaltered.

The next step in the solution of (4) is the elimination of the dependent variables, $V(R, Z)$ and $p^*(Z)$. First, the continuity equation (4a) is integrated to yield:

$$V(R, Z) = \int_R^1 \frac{\partial U^*(R', Z)}{\partial Z} \cdot dR' \tag{5a}$$

while the momentum equation is integrated over the channel cross-section to provide an expression for the pressure gradient:

$$-\frac{dp^*}{dZ} = 2\int_0^1 (U^* + U_\infty) \cdot \frac{\partial U^*}{\partial Z} \cdot dR - \frac{1}{Re} \cdot \left.\frac{\partial U^*}{\partial R}\right|_{R=1} + \frac{3}{Re} \tag{5b}$$

Equations (5) relate the transversal velocity and pressure gradient to the longitudinal velocity field, as required for completion of the integral transformation process.

Following the formalism in the generalized integral transform technique, a pair of auxiliary eigenvalue problems is selected to construct the eigenfunctions expansions, namely, for the velocity problem:

$$\frac{d^2\psi_i(R)}{dR^2} + \mu_i^2 \cdot \psi_i(R) = 0 \qquad 0 < R < 1 \tag{6a}$$

$$\left.\frac{d\psi_i(R)}{dR}\right|_{R=0} = 0 \tag{6b}$$

$$\psi_i(1) = 0 \tag{6c}$$

and for the temperature problem:

$$\frac{d^2\Gamma_i(R)}{dR^2} + \lambda_i^2 \cdot \Gamma_i(R) = 0 \qquad 0 < R < 1 \tag{7a}$$

$$\left.\frac{d\Gamma_i(R)}{dR}\right|_{R=0} = 0 \tag{7b}$$

$$\Gamma_i(1) = 0 \tag{7c}$$

Other choices of auxiliary problems were analysed in Reference 16. For the present situation of prescribed temperature boundary condition, problems (6) and (7) yield identical solutions, given by:

$$\mu_i = \lambda_i = \frac{(2i-1)}{2}\pi \tag{8a}$$

$$\psi_i(R) = \Gamma_i(R) = \cos(\mu_i \cdot R) \tag{8b}$$

and the normalization integrals:

$$N_i = \int_0^1 \psi_i^2(R)\, dR = \frac{1}{2} \tag{8c}$$

$$M_i = \int_0^1 \Gamma_i^2(R)\, dR = \frac{1}{2} \tag{8d}$$

Problems (6), (7) allow definition of the following integral transform pairs, for the velocity field:

$$\bar{U}_i^*(Z) = \frac{1}{N_i^{1/2}} \int_0^1 \psi_i(R) \cdot U^*(R, Z)\, dR, \qquad \text{transform} \tag{9a}$$

$$U^*(R,Z) = \sum_{i=1}^{\infty} \frac{1}{N_i^{1/2}} \cdot \psi_i(R) \cdot \bar{U}_i^*(Z), \qquad \text{inversion} \tag{9b}$$

and for the temperature field:

$$\bar{\theta}_i(Z) = \frac{1}{M_i^{1/2}} \int_0^1 \Gamma_i(R) \cdot \theta(R, Z)\, dR, \qquad \text{transform} \tag{10a}$$

$$\theta(R, Z) = \sum_{i=1}^{\infty} \frac{1}{M_i^{1/2}} \Gamma_i(R) \cdot \bar{\theta}_i(Z), \qquad \text{inversion} \tag{10b}$$

In terms of the transformed potentials defined by (9a) and (10a), the transversal velocity and pressure gradient are rewritten as:

$$V(R,Z)=\sum_{i=1}^{\infty}F_i(R)\cdot\frac{d\bar{U}_i^*(Z)}{dZ} \tag{11a}$$

$$-\frac{dp^*}{dZ}=2\sum_{j=1}^{\infty}\bar{U}_j^*\cdot\frac{d\bar{U}_j^*}{dZ}-\frac{1}{Re}\sum_{j=1}^{\infty}\frac{\psi_j(1)}{N_j^{1/2}}\cdot\bar{U}_j^*+\sum_{j=1}^{\infty}H_j\cdot\frac{d\bar{U}_j}{dZ}+\frac{3}{Re} \tag{11b}$$

where:

$$F_i(R)=\frac{1}{N_i^{1/2}}\cdot\int_R^1\psi_i(R')\,dR' \tag{11c}$$

$$H_j=H_j^*-3G_j \tag{11d}$$

$$H_j=\frac{1}{N_j^{1/2}}\int_0^1 U_\infty(R)\cdot\psi_j(R)\,dR \tag{11e}$$

$$G_j=\int_0^1 R\cdot F_j(R)\,dR \tag{11f}$$

Equations (4b) and (4c) are now integral transformed through the operators $\int_0^1\frac{\psi_i(R)}{N_i^{1/2}}dR$ and $\int_0^1\frac{\Gamma_i(R)}{M_i^{1/2}}dR$, respectively, to yield the transformed ordinary differential equations:

$$\mathbf{E}\frac{d\bar{\mathbf{U}}^*(Z)}{dZ}=-\mathbf{D}\bar{\mathbf{U}}^*(Z) \tag{12a}$$

$$\mathbf{A}\frac{d\bar{\theta}(Z)}{dZ}=-\mathbf{B}\bar{\theta}(Z) \tag{12b}$$

where the various coefficients matrices are given by:

$$\mathbf{E}=\{e_{i,k}\} \tag{12c}$$

$$e_{i,k}=\sum_{j=1}^{\infty}[A_{ijk}+B_{ijk}-2F_j(0)\cdot\Delta_{jk}]\cdot\bar{U}_j^*+\Delta_{jk}\cdot[Q_{ik}-F_i(0)\cdot H_k]\qquad i,k=1,2,\ldots \tag{12d}$$

$$\mathbf{D}=\{d_{i,k}\} \tag{12e}$$

$$d_{i,k}=\frac{F_i(0)}{Re}\cdot\frac{\psi_k'(1)}{N_k^{1/2}}+\Delta_{ik}\cdot\frac{\mu_i^2}{Re} \tag{12f}$$

$$\mathbf{A}=\{a_{i,j}\} \tag{12g}$$

$$a_{i,j}=\sum_{k=1}^{\infty}A_{ijk}^*\cdot\bar{U}_k^*+P_{ij}^* \tag{12h}$$

$$\mathbf{B}=\{b_{i,j}\} \tag{12i}$$

$$b_{i,j}=\frac{\Delta_{ij}}{Pe}\cdot\lambda_i^2+\sum_{k=1}^{\infty}C_{ijk}^*\cdot\frac{d\bar{U}_k^*}{dZ} \tag{12j}$$

and the various integrals are computed from:

$$A_{ijk} = = \frac{1}{N_i^{1/2} \cdot N_j^{1/2} \cdot N_k^{1/2}} \cdot \int_0^1 \psi_i(R) \cdot \psi_j(R) \cdot \psi_k(R)\, dR \tag{13a}$$

$$B_{ijk} = \frac{1}{N_i^{1/2} \cdot N_j^{1/2} \cdot N_k^{1/2}} \cdot \int_0^1 \psi_i(R) \cdot \psi_j'(R) \cdot F_k(R)\, dR \tag{13b}$$

$$Q_{ik} = Q_{ik}^* - 3S_{ik} \tag{13c}$$

$$Q_{ik}^* = \frac{3}{2} \cdot \int_0^1 (1 - R^2) \cdot \frac{\psi_i(R)}{N_i^{1/2}} \cdot \frac{\psi_k(R)}{N_k^{1/2}}\, dR \tag{13d}$$

$$S_{ik} = \frac{1}{N_i^{1/2}} \cdot \int_0^1 R \cdot \psi_i(R) \cdot F_k(R)\, dR \tag{13e}$$

$$H_k = H_k^* - 3G_k \tag{13f}$$

$$H_k^* = \frac{1}{N_k^{1/2}} \cdot \int_0^1 U_x(R) \cdot \psi_k(R)\, dR \tag{13g}$$

$$G_k = \int_0^1 R \cdot F_k(R)\, dR \tag{13h}$$

$$\Delta_{ik} = \begin{cases} 0, & \text{for } i \neq k \\ 1, & \text{for } i = k \end{cases} \tag{13i}$$

$$A_{ijk}^* = \frac{1}{M_i^{1/2} \cdot M_j^{1/2} \cdot N_k^{1/2}} \int_0^1 \Gamma_i(R) \cdot \Gamma_j(R) \cdot \psi_k(R)\, dR \tag{13j}$$

$$C_{ijk}^* = \frac{1}{M_i^{1/2} \cdot M_j^{1/2}} \int_0^1 \Gamma_i(R) \cdot \Gamma_j'(R) \cdot F_k(R)\, dR \tag{13k}$$

$$P_{ij}^* = \frac{3}{2} \cdot \left[\Delta_{ij} - \frac{1}{M_i^{1/2} \cdot M_j^{1/2}} \int_0^1 R^2 \cdot \Gamma_i(R) \cdot \Gamma_j(R)\, dR \right] \tag{13l}$$

The inlet conditions, equations (4d, lf), are similarly integral transformed to provide:

$$\bar{U}_i^*(0) = F_i(0) - H_i^*, \qquad i = 1, 2, \ldots \tag{14a}$$

$$\bar{\theta}(0) = \bar{f}_i \qquad i = 1, 2, \ldots \tag{14b}$$

where,

$$\bar{f}_i = \frac{1}{M_i^{1/2}} \int_0^1 \Gamma_i(R)\, dR \tag{14c}$$

All the integrals above are readily evaluated by analytic means. For computational purposes, the infinite systems defined by (12a,b) are truncated to sufficiently large order so as to satisfy the user requested accuracy target. In normal form, the truncated system to be numerically handled is written as:

$$\frac{d\bar{U}^*}{dZ} = -\mathbf{E}^{-1}\mathbf{D}\bar{\mathbf{U}}^* \tag{15a}$$

$$\frac{d\bar{\theta}}{\partial Z} = -\mathbf{A}^{-1}\mathbf{B}\bar{\theta} \tag{15b}$$

with inlet conditions:

$$\bar{\mathbf{U}}^*(0) = \mathbf{f}^* \tag{15c}$$

$$\bar{\theta}(0) = \mathbf{f} \tag{15d}$$

where,

$$\mathbf{f}^* = \{F_i(0) - H_i^*\} \tag{15e}$$

$$\mathbf{f} = \{\bar{f}_i\} \tag{15f}$$

Once the transformed potentials $\bar{\mathbf{U}}^*$ and $\bar{\theta}$, have been numerically evaluated at any Z of interest according to the computational procedure described in what follows, the inversion formulae are recalled to construct the original potentials, in the form:

$$U(R, Z) = U_\infty(R) + \sum_{i=1}^{N} \frac{1}{N_i^{1/2}} \cdot \psi_i(R) \cdot \bar{U}_i^*(Z) \tag{16a}$$

$$\theta(R, Z) = \sum_{i=1}^{M} \frac{1}{M_i^{1/2}} \cdot \Gamma_i(R) \cdot \bar{\theta}_i(Z) \tag{16b}$$

where N and M are the truncation orders for the velocity and temperature eigenfunction expansions, respectively.

Quantities of practical interest can then be analytically evaluated from their usual definitions, such as:

Bulk temperature

$$\theta_{av}(Z) = \frac{1}{U_m} \cdot \int_0^1 U(R, Z) \cdot \theta(R, Z)\, dR \tag{17a}$$

Local Nusselt number

$$Nu(Z) = \frac{-4 \cdot \left.\dfrac{\partial \theta}{\partial R}\right|_{R=1}}{\theta(1, Z) - \theta_{av}(Z)} \tag{17b}$$

where the temperature gradient at the wall is evaluated from the heat balance equation, for improved convergence behaviour, in the form:

$$\left.\frac{\partial \theta}{\partial R}\right|_{R=1} = Pe \cdot \frac{d}{dZ}\left[\int_0^1 U(R, Z) \cdot \theta(R, Z)\, dR\right] \tag{17c}$$

Average Nusselt number

$$Nu_{av}(Z) = \frac{1}{Z} \cdot \int_0^Z Nu(Z')\, dZ' \tag{17d}$$

COMPUTATIONAL PROCEDURE

A simple algorithm is constructed, including the attractive feature of automatically controlling the global error in the final solution for the potentials, at any selected positions (R, Z). To achieve this goal, the semi-analytic nature of this approach is employed in conjunction with well-established subroutines libraries, with thoroughly tested accuracy control schemes.

The numerical integration of system (15) is performed, for instance, through subroutine DIVPAG of the IMSL library[17] in Gear's method mode, since these ODE systems are likely to

be stiff, especially for the higher truncation orders. Since the numerical integration of the ODE systems is accomplished within user prescribed accuracy, one is left with the need of reaching convergence in the eigenfunction expansions and automatically controlling the truncation orders, N and M, for a certain number of fully converged digits requested in the final solution, at those positions of interest. The analytic nature of the inversion formulae allows for a direct testing procedure at each specified position where a solution is required, and the truncation orders, N and M, can be gradually varied to fit the global error requirements. The simple formulae for checking the accuracy is given by:

$$\varepsilon = \max_{0 \le R \le 1} \frac{\sum_{i=N^*}^{N} \frac{\psi_i(R)}{N_i^{1/2}} \cdot \bar{U}_i^*(Z)}{U_\infty(R) + \sum_{i=1}^{N} \frac{\psi_i(R)}{N_i^{1/2}} \cdot \bar{U}_i^*(Z)} \tag{18a}$$

and,

$$\varepsilon = \max_{0 \le R \le 1} \frac{\sum_{i=M^*}^{M} \frac{\Gamma_i(R)}{M_i^{1/2}} \cdot \bar{\theta}_i(Z)}{\sum_{i=1}^{M} \frac{\Gamma_i(R)}{M_i^{1/2}} \cdot \bar{\theta}_i(Z)} \tag{18b}$$

where N^* and M^* are made smaller than N or M until ε still fits the user requested precision; at this limit, either N or M are changed to assume the values of N^* or M^*, respectively. The truncation orders can also be increased and numerical integration at the last Z interval repeated, if the current values are not sufficiently large to reach the required accuracy.

Therefore, this adaptive scheme of controlling the ODE system sizes, automatically reduces computational effort and provides a global error control.

RESULTS AND DISCUSSION

First, complementing the work of Reference 15, the adaptive procedure is validated and the convergence behaviour illustrated for the velocity problem under separation of the fully developed solution, according to (3a). *Table 1* presents results of the duct centreline velocity along the dimensionless axial coordinate, for different values of the truncation order in the velocity field expansion, from $N = 5$ up to 30. Also shown are the final results achieved through implementation of the adaptive procedure, and the automatically controlled values of the system size, N. Clearly, as expected, the adaptive scheme results reproduce the fully converged solutions to within the user prescribed accuracy requirements, in this case a relative error target of 10^{-5}.

The results from the purely numerical approach[1] are also validated, demonstrating a very good agreement with the error controlled results of the present approach. It should be noted that the dimensionless axial coordinate was redefined according to the expression employed[1] for comparison purposes:

$$X^+ = \frac{z/r_w}{Re \cdot Pr} \tag{19a}$$

or,

$$X^+ = \frac{Z}{Pe} \tag{19b}$$

Table 1 Convergence analysis of duct centerline velocity and validation of adaptive procedure

	N								
X^+	5	10	15	20	25	30	Adapt.	N	Ref. 1
0.375	1.1101	1.1190	1.1221	1.1232	1.1239	1.1242	1.1242	30	1.124
0.5	1.1271	1.1386	1.1413	1.1422	1.1427	1.1430	1.1430	30	1.144
0.75	1.1609	1.1710	1.1730	1.1737	1.1740	1.1742	1.1742	30	1.177
1.0	1.1904	1.1979	1.1994	1.1999	1.2001	1.2002	1.2002	29	1.203
1.5	1.2380	1.2423	1.2432	1.2435	1.2435	1.2435	1.2435	28	1.246
2.0	1.2764	1.2690	1.2797	1.2797	1.2796	1.2796	1.2796	28	1.282
2.5	1.3092	1.3108	1.3110	1.3108	1.3107	1.3107	1.3107	28	1.312
5.0	1.4148	1.4139	1.4133	1.4129	1.4126	1.4126	1.4126	26	1.411
12.5	1.4921	1.4917	1.4914	1.4913	1.4913	1.4913	1.4913	14	1.490

Tolerance for ODE's solver: 10^{-6}
Tolerance for adaptive scheme: 10^{-5}

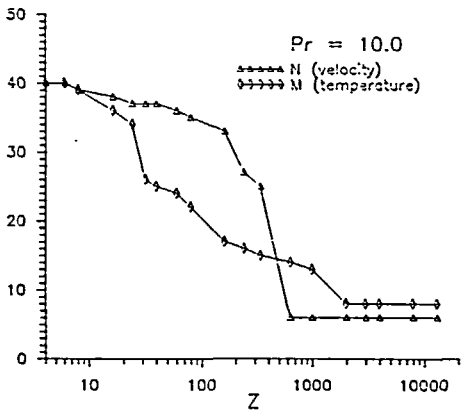

Figure 1 Reference results for local Nusselt number and validation of approximate analytical solution in Reference 16 ($Pr = 10.0$)

Figure 1 illustrates the automatic reduction on the ODE's systems sizes, for both the velocity and temperature fields, achieved through implementation of the adaptive procedure along the integration path in X^+. The temperature field is still more rapidly converging than the velocity expansion, even after separation of the fully developed flow solution. The computation represented in *Figure 1* was observed to be around 23 times faster than the numerical integration of the ODE systems with a fixed number of equations, i.e., $N = M = 40$, which confirms the marked advantages in the implementation of the adaptive procedure.

Table 2 brings a set of reference results for the fluid bulk temperature, with different values of Pr, along the duct axial coordinate. The exact fully converged results are then utilized to inspect the relative accuracy of the approximate analytic-type solutions[16], and such comparison, not possible before due to the inexistence of a truly benchmark solution, shows that the approximate solution is reasonably accurate, offering two to three digits in agreement along most of the entry region.

Table 2 Benchmark results for the fluid bulk temperature and validation of the approximate analytical solution in Reference 16

$Pr = 0.72$			$Pr = 10.0$		
χ^+	Exact	Approx.[16]	χ^+	Exact	Approx.[16]
0.0000434	0.98198	—	0.0000125	0.99445	—
0.0000868	0.97378	—	0.0000188	0.99276	—
0.000260	0.95304	0.94855	0.0000250	0.99133	—
0.000434	0.93836	0.93306	0.0000500	0.98679	—
0.000608	0.92622	0.92036	0.0000750	0.98321	—
0.000955	0.90600	0.89940	0.000100	0.98014	0.9842
0.00130	0.88893	0.88190	0.000125	0.97734	0.9821
0.00174	0.86982	0.86244	0.000188	0.97133	0.9774
0.00260	0.83764	0.82999	0.000250	0.96617	0.9733
0.00347	0.80939	0.80172	0.000500	0.94922	0.9590
0.00434	0.78391	0.77639	0.000750	0.93537	0.9464
0.00608	0.73843	0.73138	0.00106	0.92036	0.9317
0.00868	0.67910	0.67291	0.00200	0.88216	0.8924
0.0148	0.56256	0.55812	0.00313	0.84374	0.8526
0.0234	0.43346	0.43060	0.00625	0.75715	0.7644
0.0321	0.33307	0.33124	0.00938	0.68520	0.6918
0.0434	0.23657	0.23557	0.0125	0.62221	0.6284
0.0651	0.12266	0.12247	0.0250	0.43478	0.4305
0.0942	0.05082	0.05089	0.0406	0.26625	0.2689

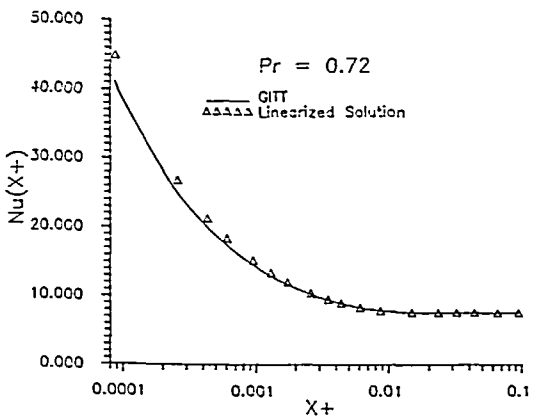

Figure 2a Automatic control of ODE's systems truncation orders through adaptive procedure

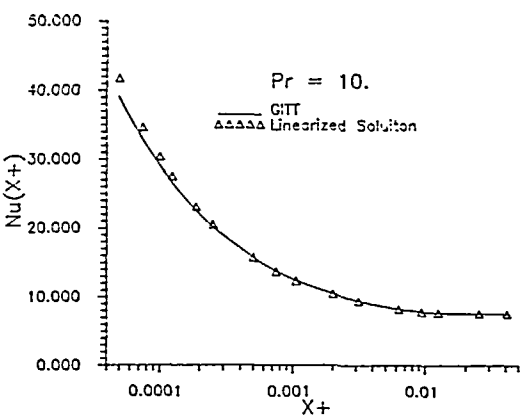

Figure 2b Reference results for local Nusselt number and validation of approximate analytical solution in Reference 16 ($Pr = 0.72$)

Figures 2a and *2b* present reference results for the local Nusselt number distributions, with different Prandtl numbers, respectively, $Pr = 0.72$ and 10. Also plotted are some results from the approximate analytical solution developed[16], based on a linearization of the velocity problem and application of the generalized integral transform technique to the resulting linear temperature problem. The agreement is quite good, except in the region close to the duct inlet, when the approximation introduced on the velocity field affects more significantly the related temperature distributions and, consequently, the Nusselt number.

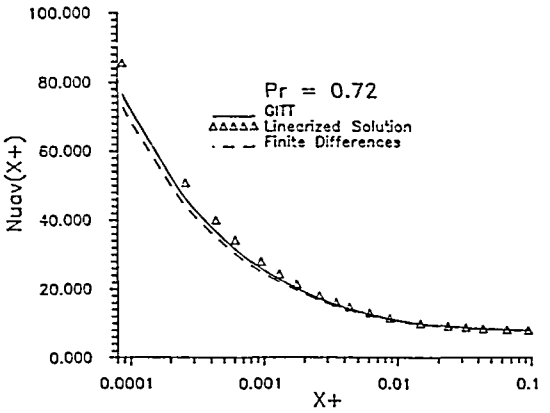

Figure 3a Average Nusselt number results and comparison with previously reported solutions ($Pr = 0.72$)

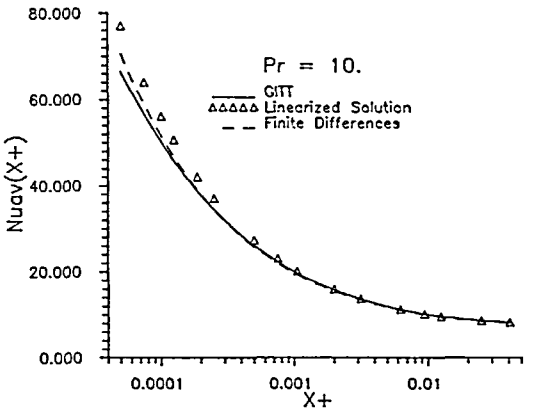

Figure 3b Average Nusselt number results and comparison with previously reported solutions ($Pr = 10.0$)

Figures 3a and *3b* show a set of benchmark results for the average Nusselt numbers in terms of the duct dimensionless length, X^+, for $Pr = 0.72$ and 10, respectively. In addition, the curves from the purely numerical solution in Reference 1 and the approximate analytical solution in Reference 16 are also plotted for the same values of Pr. The analytical solution demonstrates[16] the same trends previously discussed, while the purely numerical solutions[1] become less accurate as the inlet is approached, although not as markedly as the analytic-type solution.

The confidence built in the present application of the integral transform approach, brings the interest in considering increasingly complex problems, including the analysis of variable properties effects and different geometries.

ACKNOWLEDGEMENTS

One of the authors (R.M.C.) wishes to acknowledge the financial support provided by CNPq and the British Council, both in Brasil.

REFERENCES

1 Shah, R. K. and Bhatti, M. S. Laminar convection heat transfer in ducts, *Handbook of Single-Phase Convective Heat Transfer* (Eds. S. Kakaç, R. K. Shah and W. Aung), John Wiley, New York (1987)
2 Minkowycz, W. J., Sparrow, E. M., Schneider, G. E. and Pletcher, R. H. (Eds.), *Handbook of Numerical Heat Transfer*, John Wiley, New York (1988)
3 Kakaç, S. and Yener, Y. Laminar forced convection in the combined entrance region of ducts, in *Fundamentals of Low Reynolds Number Forced Convection* (Eds. S. Kakaç, R. K. Shah and A. E. Bergles), pp. 165–204 (1983)
4 Cotta, R. M. *Integral Transforms in Computational Heat and Fluid Flow*, CRC Press, Boca Raton, FL (1993)
5 Cotta, R. M. Hybrid numerical–analytical approach to nonlinear diffusion problems, *Num. Heat Transfer*, (*B*) *Fundamentals*, **17**, 217–226 (1990)
6 Serfaty, R. and Cotta, R. M. Integral transform solutions of diffusion problems with nonlinear equation coefficients, *Int. Commun. Heat & Mass Transfer*, **17**, 851–867 (1990)
7 Diniz, A. J., Aparecido, J. B. and Cotta, R. M. Heat conduction with ablation in a finite slab, *Int. J. Heat Technol.*, **8**, 30–43 (1990)
8 Cotta, R. M. and Serfaty, R. Integral transform algorithm for parabolic diffusion problems with nonlinear boundary and equation source terms, *7th Int. Conf. Num. Meth. Thermal Problems, Stanford*, Vol. II, pp. 916–926 (1991)
9 Leiroz, A. J. K. and Cotta, R. M. On the solution of nonlinear elliptic convection–diffusion problems through the integral transform method, *Num. Heat Transfer*, (*B*) *Fundamentals*, **23**, 401–411 (1992)

10 Serfaty, R. and Cotta, R. M. Hybrid analysis of transient nonlinear convection–diffusion problem, *Int. J. Num. Meth. Heat Fluid Flow*, **2**, 55–62 (1992)
11 Pérez Guerrero, J. S. and Cotta, R. M. Integral transform method for Navier–Stokes equations in stream function-only formulation, *Int. J. Num. Meth. Fluids*, **15**, 399–409 (1992)
12 Boahua, C. and Cotta, R. M. Integral transform analysis of natural convection in porous enclosures, *Int. J. Num. Meth. Fluids*, **17**, 787–801 (1993)
13 Cotta, R. M., Pérez Guerrero, J. S. and Scofano Neto, F. Hybrid solution of the incompressible Navier–Stokes equations via integral transformation, *2nd Int. Conf. on Adv. Computat. Meth. in Heat Transfer* (*HEAT TRANSFER 92*), *Milan*, Vol. 1, pp. 735–750 (1992)
14 Mikhailov, M. D. and Cotta, R. M. Unified integral transform method, *J. Braz. Ass. Mech. Sci., RBCM*, **12**, 301–310 (1990)
15 Cotta, R. M. and Carvalho, T. M. B. Hybrid analysis of boundary layer equations for internal flow problems, *7th Int. Conf. Num. Meth. Lamin. & Turbul. Flow, Stanford*, Vol. I, pp. 106–115 (1991)
16 Campos Silva, J. B., Cotta, R. M. and Aparecido, J. B. Analytical solution to simultaneously developing laminar flow inside parallel-plates channel, *Int. J. Heat Mass Transfer*, **35**, 887–895 (1992)
17 IMSL Library, MATH/LIB, Houston, TX (1987)